

UNCLASSIFIED

Defense Technical Information Center  
Compilation Part Notice

ADP019128

TITLE: Fracture and Residual Characterization of Tungsten Carbide Cobalt Coatings on High Strength Steel

DISTRIBUTION: Approved for public release, distribution unlimited

This paper is part of the following report:

TITLE: International Conference on the Mechanical Behavior of Materials [9th], ICM-9, Held in Geneva, Switzerland on 25-29 May 2003

To order the complete compilation report, use: ADA433037

The component part is provided here to allow users access to individually authored sections of proceedings, annals, symposia, etc. However, the component should be considered within the context of the overall compilation report and not as a stand-alone technical report.

The following component part numbers comprise the compilation report:

ADP018903 thru ADP019136

UNCLASSIFIED

# **FRACTURE AND RESIDUAL STRESS CHARACTERIZATION OF TUNGSTEN CARBIDE COBALT COATINGS ON HIGH STRENGTH STEEL**

Donald S. Parker

Structural Materials Engineer, NASA, Kennedy Space Center, Florida, USA

[donald.s.parker@nasa.gov](mailto:donald.s.parker@nasa.gov)

Thomas R. Watkins, PhD

Oak Ridge National Laboratory, Oak Ridge, Tennessee, USA

[watkinstr@ornl.gov](mailto:watkinstr@ornl.gov)

O. Burl Cavin

Oak Ridge National Laboratory, Oak Ridge, Tennessee, USA

[cavino@ornl.gov](mailto:cavino@ornl.gov)

Darryl P. Butt, PhD

University of Florida, Gainesville, Florida

[dbutt@mse.ufl.edu](mailto:dbutt@mse.ufl.edu)

## **ABSTRACT**

Tungsten carbide cobalt coatings applied via high velocity oxygen fuel thermal spray deposition are essentially anisotropic composite structures with aggregates of tungsten carbide particles bonded with both amorphous and crystalline cobalt phases. X-ray diffraction was used to characterize the residual stresses within the coatings to understand the crack initiation and propagation behavior of samples subjected to axial fatigue loads. Diffraction was also used to establish a baseline stress state of the uncoated high strength steel fatigue specimens. Stress states were evaluated for bare metal, and coated hourglass fatigue specimens that were subjected to low, medium and high cyclic fatigue conditions. Scanning electron microscopy was used to determine coating crack initiation and propagation paths within the coating as well as substrate fatigue site origins. After finish grinding, observed coating cracks were determined to have started at surface defects and were observed to propagate in the radial direction towards the substrate along splat and interfacial boundaries within the softer cobalt coating matrix. These boundaries provide paths for cracks around WC particles, which contain high compressive residual stresses. High magnification inspection also confirmed that substrate fatigue cracks initiate at subsurface inclusions when subjected to low stress conditions and substrate-coating interface defects when subjected to high stress conditions. Subsurface defects are inclusions and impurities from the steel manufacturing process whereas the interfacial defects are imbedded aluminum oxide particles from the grit blasting process used to prepare the substrate surface for coating application. Cracks in the coating from applied axial stresses do not propagate beyond the coating-substrate interface and did not provide preferential sites for substrate fatigue crack initiation.

## **INTRODUCTION**

Tungsten carbide cobalt materials have been widely used historically to protect surfaces from both adhesive and abrasive wear in many different aerospace applications. Specifically, the thermal sprayed, high velocity oxygen fuel (HVOF) tungsten carbide cobalt coatings provide the highest wear resistance in rolling or sliding contact wear

applications. HVOF coatings are applied by feeding a uniform sized powder into a combustion plume. The molten and semi-molten globules are projected through a supersonic jet stream onto a substrate. The resulting coating has a lamellar grain structure of interlocking cobalt phase “splats” resulting from the impact and rapid solidification of these globules. The Co splats contain distributed carbide particles.

For landing gear and hydraulic components in aerospace applications, the beneficial wear properties of the HVOF sprayed tungsten carbide cobalt coatings are very attractive as compared to other materials. However, durability of the brittle coatings in fatigue sensitive areas is a concern. Critical to the application of these coatings is understanding the stress conditions under which coating cracks can form, the method and direction of crack propagation, and what effect these coating cracks have on initiation of substrate fatigue cracks.

Residual stress is defined as the stress that remains in a material that is at equilibrium with its surroundings without any sustained applied loads. Surface macrostresses are often induced to counteract solidification or thermal tensile stresses, or to reduce the localized susceptibility for fatigue crack initiation. For example, high strength steels are shot-peened to impart a compressive residual stress at the surface to mitigate the effect of tensile surface stresses from manufacturing processes. However, when HVOF coatings are applied, the surface must be grit blasted to form a coarse surface profile for optimum coating adhesion. This can adversely affect the compressive residual stress state of the shot-peened layer and possibly the resistance to fatigue crack initiation. X-ray diffraction techniques, which measure the *total* strain, can be used to characterize surface stresses non-destructively by calculating the elastic strains,  $\epsilon$ , through the change in the Bragg scattering angle,  $\Delta\theta_B$ , as follows:

$$\lambda = 2d \sin \theta_B, \quad (1)$$

where  $\lambda$  is the wavelength of the radiation,  $d$  is the interplanar spacing and  $\theta_B$  is the Bragg angle. Solving for strain:

$$\epsilon = (d_1 - d_0) / d_0, \quad (2)$$

where  $d_1$  and  $d_0$  are the stressed and stress free interplanar spacings, respectively. The strains can be converted to stress using the appropriate tensor equations and for metals and coatings. This can provide a very accurate determination of the residual stress values. One of the limitations of this technique is the shallow penetration depth of the x-ray beam, with roughly half of the diffracted radiation originating from a depth of less than 0.0004” beneath the surface, which restricts evaluation to the near surface region. However, understanding the near surface stress behavior is important to understand fatigue crack formation and propagation. Measurement of stress values associated with known constituents within a coating and along the substrate surface can provide a relative understanding of the internal stress state of the individual phases and particles and their relationship to crack initiation and propagation. For coating materials, internal regions of tensile and compressive stress will tend to direct the crack path and the propagation rate of a coating fracture. [2].

## EXPERIMENTAL PROCEDURE

Standard hourglass fatigue specimens were manufactured from a common landing gear alloy material, AISI 4340, heat-treated to 280-300 ksi tensile strength and shot-

peened to an intensity of 8-12A with S230 wrought steel shot. The gage section was grit blasted with 54 grit aluminum oxide at 60-80 psi with an 8" standoff distance and then coated with HVOF, thermal sprayed WC-17 wt.% Co coating using parameters optimized for maximum fatigue life. The coating was finish ground and polished between centers to 0.003" thickness and a surface roughness of 2-4  $R_a$ .

Baseline  $\theta/2\theta$  scans were run on a bare metal, shot-peened sample, a shot-peened and grit blasted specimens, a coated specimen as-sprayed, and a coated specimen that had been finish ground. Virgin WC-17 wt.% Co powder, and virgin WC powder were also scanned to provide a baseline unstressed lattice spacing for the coating materials. The residual stresses were also determined for representative specimens subjected to axial fatigue stresses with the following conditions: shot-peened and grit blasted high strength steel, coated and finish ground with WC-17 wt.% Co then tested at 110ksi maximum applied stress, 150ksi maximum applied stress, and 220ksi maximum applied stress.

Table I lists the details of the experimental conditions for the x-ray measurements. Briefly, a 4-axis ( $\Phi$ ,  $\chi$ ,  $\Omega$ ,  $2\Theta$ ) goniometer was employed for the stress measurements using the " $\Psi$ -goniometer geometry" [4] using parallel beam optics, which removes sample surface displacement errors [5]. Due to the absence of overlapping peaks, the (211) and (103) reflections from the WC were utilized for the strain measurement and were located at  $\sim 117^\circ$  and  $121^\circ 2\Theta$ , respectively. No strains were measured from the matrix as no reflections from the matrix were available in the needed high  $2\Theta$  region. Specimen alignment was accomplished using a dial gauge probe, which was accurate to  $\pm 5 \mu\text{m}$ . Here, the relative distance to the center of rotation is known, and the diffracting surface is positioned accordingly. The average strain free interplanar spacing,  $d_0$ , was determined from the x-ray data employing the analysis of Hauk et al. [4]. Goniometer alignment was ensured by examining  $\text{LaB}_6$  powder on a zero background plate. The maximum observed peak shift for the (510) reflection of  $\text{LaB}_6$  ( $141.7^\circ 2\Theta$ ) was less than  $0.01^\circ 2\Theta$  for  $\chi$  tilting as described in Table I. The stresses were calculated using the Dölle-Hauk method [4] assuming a triaxial stress state. Values for Poisson's ratio and Young's moduli for the (211) and (103) WC reflections were calculated [7,8] from single crystal elastic constants [9] to be 92,679ksi (639 GPa) and 199,656 ksi (825 GPa), respectively.

Table 1-Experimental conditions for the x-ray measurements.

Parameter	Condition
Equipment	MAC Science 18 kW rotating anode generator Osmic CMF multilayer mirror Scintag PTS goniometer Scintag liquid $\text{N}_2$ -cooled Ge detector
Power	8 kW; 40 kV, 200 mA
Radiation	Cu, $\lambda = 1.54059 \text{ \AA}$
Incidence slit width	0.5 mm
Receiving slit acceptance	$0.25^\circ$ ; radial divergence limiting (RDL) Soller slit
Source to specimen distance	360 mm
Specimen to back slit distance	280 mm
Tilt axis and angles	$\chi$ ; $0, \pm 28.2, \pm 42, \pm 55^\circ$ (equal steps of $\sin^2 \psi$ )
Scans	$115^\circ \leq 2\theta \leq 123^\circ 2\theta$ , $0.02^\circ 2\theta/\text{step}$ ; 10 s/step

Scanning electron microscopy was performed on the fractured fatigue test specimens using a JEOL JSM 5900LV. The specimens were evaluated at various magnifications to evaluate coating surface morphology, coating crack origin analysis, coating fracture surface feature identification, and substrate fatigue crack origin analysis.

## RESULTS AND DISCUSSION

### Residual Stress Analysis

In Figure 1, a baseline scan of a coated specimen shows the presence of WC and Co phases. The cobalt reflections were not all observed due in part to its low volume fraction, low atomic number and superposition with an amorphous hump between 30 and 50 degrees  $2\theta$ . The amorphous hump is a metastable phase consisting of ternary Co, W, and C that formed due to the rapid undercooling. As a result, the residual stress analysis was performed using the 117 and 120 degrees  $2\theta$  reflections for WC since they possessed reasonable intensity and no overlapping peaks.

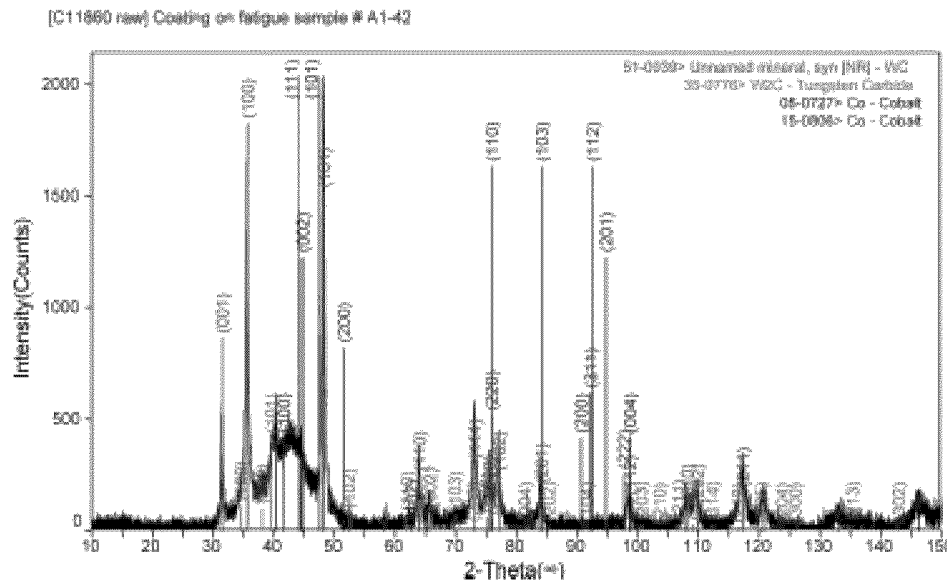


Figure 1. Theta/2-theta scan results for a coated specimen.

The residual stress results are given in Table 2. For the bare metal shot-peened specimens, the calculated values showed compressive residual stress in all three axes, with the radial direction being the lowest value. Once the substrates were grit blasted with aluminum oxide, the surface residual stress state was altered, as expected from the change in surface morphology of a smooth dimpled appearance to a coarse surface. Here, the impacting grit particles act to increase the compressive peening effect on the stress in

the axial direction while relieving some of the near surface stresses in other directions (see Table 2) [5].

Next, the surface residual stress of WC particles within the as-sprayed coated specimen was determined to be in 3-D compression prior to fatigue testing. The coated specimens were then ground and polished to a 2-4 Ra surface finish, and re-examination showed a significant increase in compressive stresses in both the axial and hoop directions with a reduction in the radial direction. This indicates that the grinding and polishing process used to achieve the desired surface finish has a significant effect on the residual coating stresses in the near surface region. Although elastic constant differences have been accounted for, the residual stresses for the two reflections are not the same, but similar due in part to the differences in strain sensitivity and the discontinuous sampling nature of x-ray diffraction. That is, a different set of grains is diffracting for the (211) than for the (103); each set is likely experiencing a slightly different residual stress.

<u>Condition</u>	<u>Axial</u>	<u>Hoop</u>	<u>Radial</u>
4340 steel substrate			
Shot-peened *	-133 ksi	-137 ksi	-22 ksi
Shot-peened & Al <sub>2</sub> O <sub>3</sub> grit blasted **	-154 ksi	-89 ksi	-3.1 ksi
As-sprayed WC-17wt.%Co			
(211) reflection	-85 ksi	-116 ksi	-99 ksi
(103) reflection	-50 ksi	-73 ksi	-76 ksi
Finish ground & Polished			
(211) reflection	-264 ksi	-224 ksi	-33 ksi
(103) reflection	-193 ksi	-245 ksi	-22 ksi
Fatigue Tested at 110 ksi			
(211) reflection	-158 ksi	-146 ksi	-12 ksi
(103) reflection	--	--	--
Fatigue Tested at 150 ksi			
(211) reflection	-280 ksi	-215 ksi	-21 ksi
(103) reflection	-140 ksi	-130 ksi	+27 ksi
Fatigue Tested at 220 ksi			
(211) reflection	-219 ksi	-125 ksi	-32 ksi
(103) reflection	-100 ksi	-33 ksi	-25 ksi

\*peened using S230 shot to an intensity of 8-12A, verified by Almen "A" deflection strip as 11.3; \*\* blasted with 54 grit aluminum oxide prior to HVOF coating

Table 2 –Residual stresses for the specimens examined.

The coated 4340 steel specimen subjected to high cycle fatigue testing at low maximum applied stresses loads (110ksi) showed decreased compressive residual coating stresses in all three axes for the (211) reflection, relative to the ground and polished sample. This result was most likely due to relaxation of the residual stresses during the elastic deformation experienced during fatigue testing which acts to relieve the effect of stresses imparted during the surface finishing operation. The 4340 specimens tested in

this range did not fracture and were run-out specimens that reached  $10^7$  cycles so both the coating and substrate experienced significant elastic strain. The coatings only showed very fine cracks distributed across the surface that were not interconnected and were likely the result of interlamellar plastic deformation of the cobalt binder [6]. Unlike the other coated specimens, the (103) reflections were of exceptionally low intensity, making peak position determination difficult and unreliable. A linear-line force fit to the resulting  $\sin^2\psi$  plots was unsatisfying given the oscillatory nature of the data and further gave tensile strains. As this result was judged to be flawed, the stress values were not reported.

The residual stresses of the specimen subjected to fatigue testing at medium applied stresses loads (150ksi) were similar to those of the ground and polished specimen for the (211) reflection, but larger in magnitude than those for the 110ksi specimen. The (103) reflection results suggested a reduction in compressive stress after fatigue testing at medium applied stresses loads relative to the ground and polished specimen. The coated 4340 steel specimen fatigue tested the highest stress level of 220ksi maximum applied stress was evaluated at a section of coating adjacent to a delaminated region on the same side as the fracture surface origin. The compressive stresses were lower than the 150ksi specimen for the axial and hoop directions for both reflections (see Table 2). The difference in stresses values between the (211) and (103) reflections increased further perhaps suggesting microstructural changes preferentially affecting the (103) planes.

### Optical and Scanning Electron Microscopy

Cracks in WC wt. 17% Co high velocity oxygen fuel (HVOF) thermal spray coatings subjected to axial fatigue stresses initiate at defects in the coating structure at the surface, and propagate along intersplat regions within the coating structure, avoiding the compressively stressed WC particles as shown in Figure 2. The direction of crack propagation is in the radial direction, perpendicular to the axis of loading.

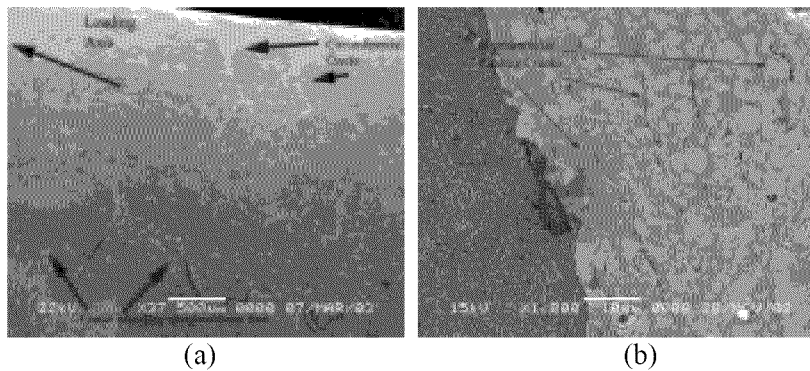


Figure 2. Images showing: (a) the coating surface cracks after fatigue testing and (b) a polished cross-section of the tungsten carbide cobalt coating with interlamellar cracks propagating along phase boundaries around the white carbide particles.

Microscopic examination of cross-sections and fracture surfaces showed that when the deep coating cracks either propagate along the bond-line interface or turn back into the coating and propagate along splat boundaries in the first few layers of deposited coating as shown in Figure 3. High magnification scanning electron microscopy of the fatigue specimens fracture surface clearly showed that the substrate fatigue crack origins were located at either a subsurface inclusion, or at a coating-substrate interfacial bond line defect. The subsurface defects (see Figure 4A) were the predominant mode of initiation at applied fatigue stresses below 150ksi; the longer fatigue life indicates that the properties of the substrate controlled fatigue initiation. Whereas, for the specimens tested above 150ksi maximum applied stresses, substrate-coating interface defects predominated as the substrate fatigue site origin (see Figure 4B). Energy dispersive spectroscopy confirmed that the defects at the coating-substrate interface were imbedded aluminum oxide particles from the grit blasting operation prior to coating deposition. The subsurface defects could not be identified but could be  $M_2C$  carbide particles at grain boundaries or sulfur inclusions in the matrix [6].

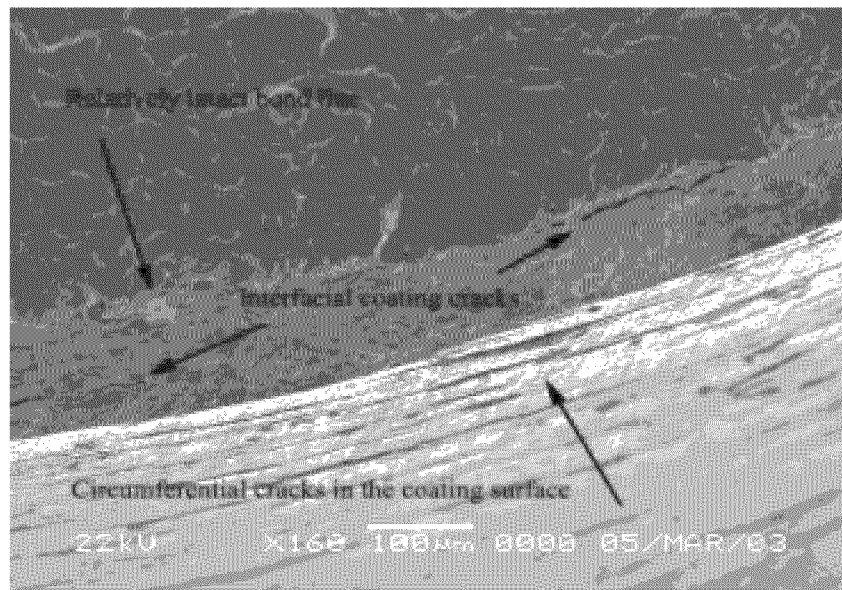


Figure 3. SEM micrograph showing the coating cracks at the substrate bond-line interface.



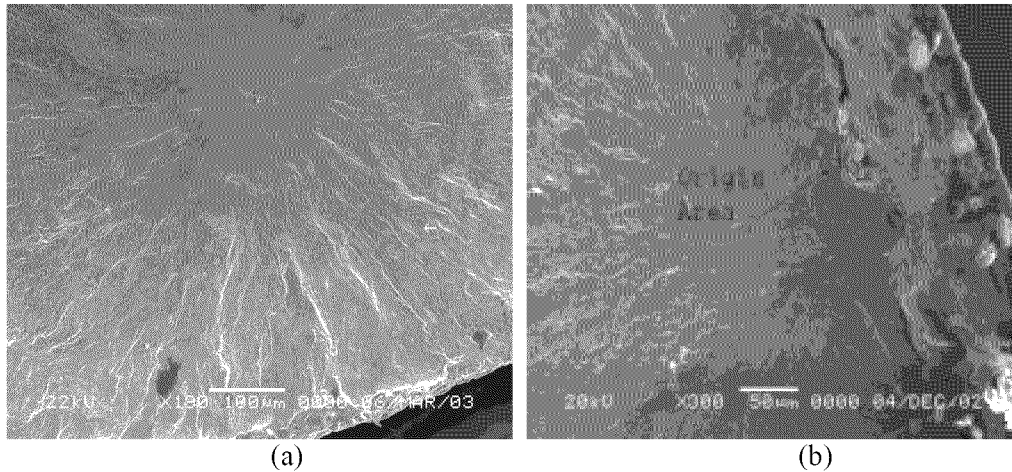


Figure 4. SEM Micrographs showing: (a) subsurface origin in a 4340 specimen tested at 150ksi maximum applied stress, and (b) surface origin at an aluminum oxide particle in a 4340 specimen tested at 220ksi maximum applied stress

## SUMMARY

X-ray residual stress measurements showed that the grit blasting process prior to coating application reduced the compressive residual stress state of the shot-peened substrate. Analysis of the HVOF applied coatings showed that the tungsten carbide particles were in compression within the cobalt matrix, and at low to moderate applied axial stress levels, fatigue crack initiation was controlled by the substrate properties. At higher applied axial fatigue stresses, the beneficial effects of substrate shot-peening are overcome likely due to elastic and plastic deformation which acts to free up dislocation motion at the cold worked surface. With the beneficial residual stress reduced in the coating and likely in the substrate, substrate-coating bond-line defects provide sufficient stress concentrations for fatigue crack initiation [5] [6].

## REFERENCES

- [1] P. Whithers and H. Bhadeshia, "Residual Stress," in *Journal of Materials Science and Technology*, Vol. 17, pp 355-375, April 2001, IoM Communications Ltd.
- [2] P.S. Prevey, "Problems with Non-destructive Surface X-ray Diffraction Residual Stress Measurement," in *Practical Applications of Residual Stress Technology*, pp. 47-54 ASM Int'l, 1991, C. Ruud Editor.
- [3] M. Nascimento, R.C. Souza, I.M. Miguel, W.L. Pigatin, and H.J.C. Voorwald, "Effects of Tungsten Carbide Thermal Spray Coating by HP/HVOF and Hard Chromium

Electroplating on AISI 4340 High Strength Steel,” in Surface and Coatings Technology 138, pp. 113-124, 2001, Elsevier Science B.V.

[4] I.C. Noyan and J.B. Cohen, Residual Stress, Measurement by Diffraction and Interpretation, Springer-Verlag, New York, 1987, pp. 102 and 125-130.

[5] P.S. Prevey, "X-ray Diffraction Characterization of Residual Stresses Produced by Shot Peening," in Shot Peening, Theory and Application, pp. 81-93, IITT-International, 1990, A. Niku-Lari Editor.

[6] D.S. Parker " Fracture and Residual Stress Characterization of Tungsten Carbide 17% Cobalt Thermal Spray Coatings Applied to High Strength Steel Fatigue Specimens," Masters Thesis, University of Florida, 2003.

[7] J. F. Nye, Physical Properties of Crystals, Clarendon Press, Oxford, 1985, p. 147.

[8] B. D. Cullity, Elements of X-ray Diffraction, 2<sup>nd</sup> ed, Addison-Wesley, Reading, MA, 1978, p. 502.

[9] M. Lee and R. S. Gilmore, “Single Crystal Elastic Constants of Tungsten Monocarbide,” J. Mat. Sci. **17** 2657-2660 (1982).

## **ACKNOWLEDGEMENTS**

Research sponsored by the Assistant Secretary for Energy Efficiency and Renewable Energy, Office of FreedomCAR and Vehicle Technologies, as part of the High Temperature Materials Laboratory User Program, Oak Ridge National Laboratory, managed by UT-Battelle, LLC, for the U.S. Department of Energy under contract number DE-AC05-00OR22725.